Robotica (2005) volume 23, pp. 83–91. © 2005 Cambridge University Press
DOI: 10.1017/S0263574704000578 Printed in the United Kingdom

# Jamming analyses for dual peg-in-hole insertions in three dimensions

Yanqiong Fei and Xifang Zhao

*Research Institute of Robotics, Shanghai Jiao Tong University, Huashan Road 1954, Shanghai 200030 (P. R. of China) E-mail: fyq@sjtu.edu.cn*

(Received in Final Form: May 20, 2004)

**SUMMARY**

In this paper, jamming analyses of the three dimensional dual peg-in-hole are presented. First, for a three dimensional dual peg-in-hole, possible contact states are enumerated and geometric analyses are presented. Second, the contact forces are described by the screw theory in three dimensions. The force/moment equations for static equilibrium states of three dimensional dual-peg insertions are derived. Third, jamming diagrams are obtained. Eleven kinds of possible jamming diagrams are analyzed. Finally, an experiment of a dual peg-in-hole assembly is presented to show the effectiveness of the above analyses.

KEYWORDS: Robot automatic assembly; Dual peg-in-hole; Jamming; Three dimensions

## 1. INTRODUCTION

Analyses of the physics of robot assembly tasks are important in developing a flexible assembly system. Assembly analyses involve those of force/moments due to contacts and jamming conditions due to improper force/moments.

Because of the uncertainty of geometry and control, contact states exist during the assembly process. Xiao[1] presented the notion of contact formation (CF) in terms of principal contacts (PCs) to characterize contact states, and defined contact states as CF-connected regions of contact configurations. He also examined the neighboring relations between contact states and characterized the contact state space as a contact state graph. Xiao[2] developed an algorithm that automatically generated a high-level contact state graph and planned contact motions between two known adjacent contact states.

Force/moment analysis is an important element in robot assembly analyses. Much research has been done on single peg-in-hole insertions. Simunivic[3] analyzed a round peg insertion problem, and derived two dimensional single peg-in-hole jamming conditions. Whitney[4] adopted Simunovic's approach to determine the force analysis of the same problem. He identified wedging and jamming conditions and recommended ways to avoid insertion failure. A compliant mechanism, RCC (Remote-Center-Compliance) was designed for axi-symmetric part insertions. Sturges and Laowattana analyzed the wedging condition in rectangular peg insertion[5,6] and developed a Spatial Remote-Center-Compliance (SRCC).[7] Tsaprounis[8] focused on the determination of forces at contact points between a round peg and a hole.

Many theories have also been studied over the past years that define two dimensional mating between double rigid cylindrical parts.[9–11] Sturges[11] analyzed two dimensional dual peg-in-hole insertion problems. Jamming diagrams of a two dimensional dual peg-in-hole insertion were obtained.

At present, research activities in the area concentrated on:

(i) Three dimensional multiple peg-in-hole analyses
(ii) Modeling of contact
(iii) Design of assembly devices

Multiple peg-in-hole insertions represent a class of practical and complicated tasks in the field of robotic automatic assembly. Because of the difficulty and complexity in analyzing three-dimensional multiple peg-in-hole insertions, most of the analyses of this class of assembly tasks to date were done by simplifying the problems into two dimensions.[9–11] Analyses of the dual peg-in-hole problem in three dimensions are few.[12] Sturges' work on the three-dimensional analysis of multiple-peg insertion gives an insight into the behavior of the pegs during the chamfer-crossing phase of the problem.[13] Fei's geometric analysis of a triple peg-in-hole insertion forms the base of three-dimensional assembly problems.[14]

However, for three dimensional multiple peg-in-hole insertion tasks, there is not yet a perfect assembly theory and experimental analyses at present. After analyzing multiple peg-in-hole insertions in three dimensions, the whole assembly process and its complexity and difficulty can be known in detail. Thus, some simple and special machines can be designed to finish this type of tasks.

In the paper, a complete contact and jamming analysis of dual peg-in-hole insertion needs to be done in three dimensions. By understanding the physics of three dimensional assembly processes, one can plan find motion strategies and guarantee successful operations.

Firstly, all possible contact states are enumerated in three dimensions. Secondly, contact forces can be described by the screw theory. Applying the static equilibrium equations, the conditions on applied forces and moments for maintaining each contact state are formulated. Thirdly, jamming diagrams are obtained. The force/moment conditions to guarantee successful insertion are obtained from all possible jamming diagrams. Then, some contact states are given, which finish the dual peg-in-hole process. Their geometric conditions are

https://doi.org/10.1017/S0263574704000578 Published online by Cambridge University Press

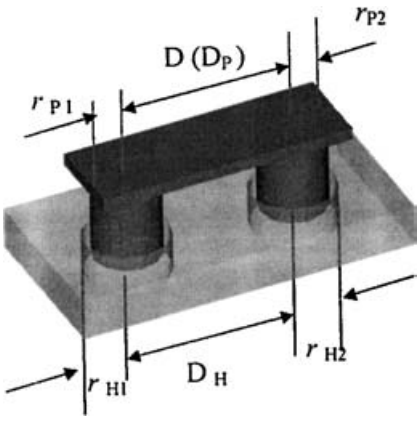



Fig. 1. Geometry of a dual peg-in-hole.

derived. After these analyses, an experiment of the dual peg-in-hole insertion is presented and the result is shown.

## 2. CONTACT STATES CLASSIFICATION OF DUAL PEG-IN-HOLE IN THREE DIMENSIONS

The geometric model of a dual peg-in-hole problem is shown in Fig. 1. The left peg has a radius of $r_{P1}$, whereas the right peg has a radius of $r_{P2}$. The radii of left hole and right hole are $r_{H1}$ and $r_{H2}$, respectively. D ($D_P$) represents the distance between the peg axes, and $D_H$ represents the distance between the hole axes. The clearances between left peg and left hole, and between right peg and right hole are $c_1$ and $c_2$, respectively. To simplify our analyses, we only consider multiple pegs which are round, parallel and have the same length. Besides these, we make the following assumptions: (i) In the assembly process, the angle between the axes of the pegs and those of the holes is small and can be neglected; (ii) Insertion direction is only vertically downward; (iii) Quasi-static motion; (iv) All axes of the holes are parallel to each other, and perpendicular to the horizontal plane; (v) The clearances between pegs and holes are positive.

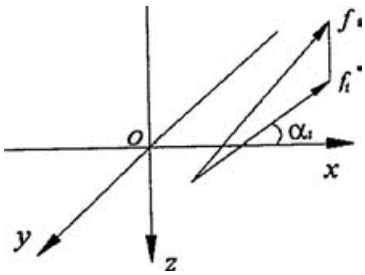



Fig. 2. $\alpha_i$ between the vector $f_i^*$ and the x-axis.

Because of the uncertainty of geometry and control, contact states exist during the assembly process. For a dual peg-in-hole insertion, three-point contact states exist only when a certain set of conditions are satisfied. Three-point contact states or four-point contact states are transient and considered trivial.[11] Thus, in the paper, one-point and two-point contact states will be analyzed in detail.

There are ten kinds of contact states when pegs tilt to the left, as shown in Table I. The coordinate system oxyz is set up at the center of dual pegs. Here $i = 1$ represents that of the left peg and left hole contact in the left, $i = 2$ represents that of the left peg and left hole contact in the right, $i = 3$ represents that of the right peg and right hole contact in the left, $i = 4$ represents that of the right peg and right hole contact in the right. Mapping the contact force $f_i$ to the plane xoy, the corresponding vector $f_i^*$ can be obtained; $\alpha_i$ is an angle between the vector $f_i^*$ and the x-axis (Fig. 2). According to the above assumption, $\theta$ is small and can be neglected. Thus, $f_i^*$ is equal to $f_i$; $r_i$ is a vector which represents contact point's position in fixed coordinate system oxyz; $h_i$ is an insertion depth; $\mu$ is friction coefficient. According to the above analysis, there are also ten kinds of contact states when pegs tilt to the right (Table I).

Table I. Assembly contact states of a dual peg-in-hole in three dimensions.

| Dual peg-in-hole | Three dimensional contact states | $\alpha_i$ | $r_i$ |
|---|---|---|---|
| When pegs tilt to the left, | One-point contact states | | |
| $k$ stands for $l$. | ($k$-1) | $\alpha_1 \in [0^\circ \quad 90^\circ] \cup [270^\circ \quad 360^\circ]$ | $r_1 : (x_1 \quad y_1 \quad -jh_1)$ |
| | ($k$-2) | $\alpha_2 \in [90^\circ \quad 270^\circ]$ | $r_2 : (x_2 \quad y_2 \quad -(1-j)h_2)$ |
| | ($k$-3) | $\alpha_3 \in [0^\circ \quad 90^\circ] \cup [270^\circ \quad 360^\circ]$ | $r_3 : (x_3 \quad y_3 \quad -jh_3)$ |
| | ($k$-4) | $\alpha_4 \in [90^\circ \quad 270^\circ]$ | $r_4 : (x_4 \quad y_4 \quad -(1-j)h_4)$ |
| When pegs tilt to the right, | Two-point contact states | | |
| $k$ stands for $r$. | ($k$-5) | $\alpha_1 \in [0^\circ \quad 90^\circ] \cup [270^\circ \quad 360^\circ]$, $\alpha_2 \in [90^\circ \quad 270^\circ]$ | $r_1 : (x_1 \quad y_1 \quad -jh_1)$, $r_2 : (x_2 \quad y_2 \quad -(1-j)h_2)$ |
| | ($k$-6) | $\alpha_3 \in [0^\circ \quad 90^\circ] \cup [270^\circ \quad 360^\circ]$, $\alpha_4 \in [90^\circ \quad 270^\circ]$ | $r_3 : (x_3 \quad y_3 \quad -jh_3)$, $r_4 : (x_4 \quad y_4 \quad -(1-j)h_4)$ |
| | ($k$-7) | $\alpha_1 \in [0^\circ \quad 90^\circ] \cup [270^\circ \quad 360^\circ]$, $\alpha_3 \in [0^\circ \quad 90^\circ] \cup [270^\circ \quad 360^\circ]$ | $r_1 : (x_1 \quad y_1 \quad -jh_1)$, $r_3 : (x_3 \quad y_3 \quad -jh_3)$ |
| | ($k$-8) | $\alpha_1 \in [0^\circ \quad 90^\circ] \cup [270^\circ \quad 360^\circ]$, $\alpha_4 \in [90^\circ \quad 270^\circ]$ | $r_1 : (x_1 \quad y_1 \quad -jh_1)$, $r_4 : (x_4 \quad y_4 \quad -(1-j)h_4)$ |
| | ($k$-9) | $\alpha_2 \in [90^\circ \quad 270^\circ]$, $\alpha_3 \in [0^\circ \quad 90^\circ] \cup [270^\circ \quad 360^\circ]$ | $r_2 : (x_2 \quad y_2 \quad -(1-j)h_2)$, $r_3 : (x_3 \quad y_3 \quad -jh_3)$ |
| | ($k$-10) | $\alpha_2 \in [90^\circ \quad 270^\circ]$, $\alpha_4 \in [90^\circ \quad 270^\circ]$ | $r_2 : (x_2 \quad y_2 \quad -(1-j)h_2)$, $r_4 : (x_4 \quad y_4 \quad -(1-j)h_4)$ |

When pegs tilt to the left, $j = 1$. When pegs tilt to the right, $j = 0$.

https://doi.org/10.1017/S0263574704000578 Published online by Cambridge University Press

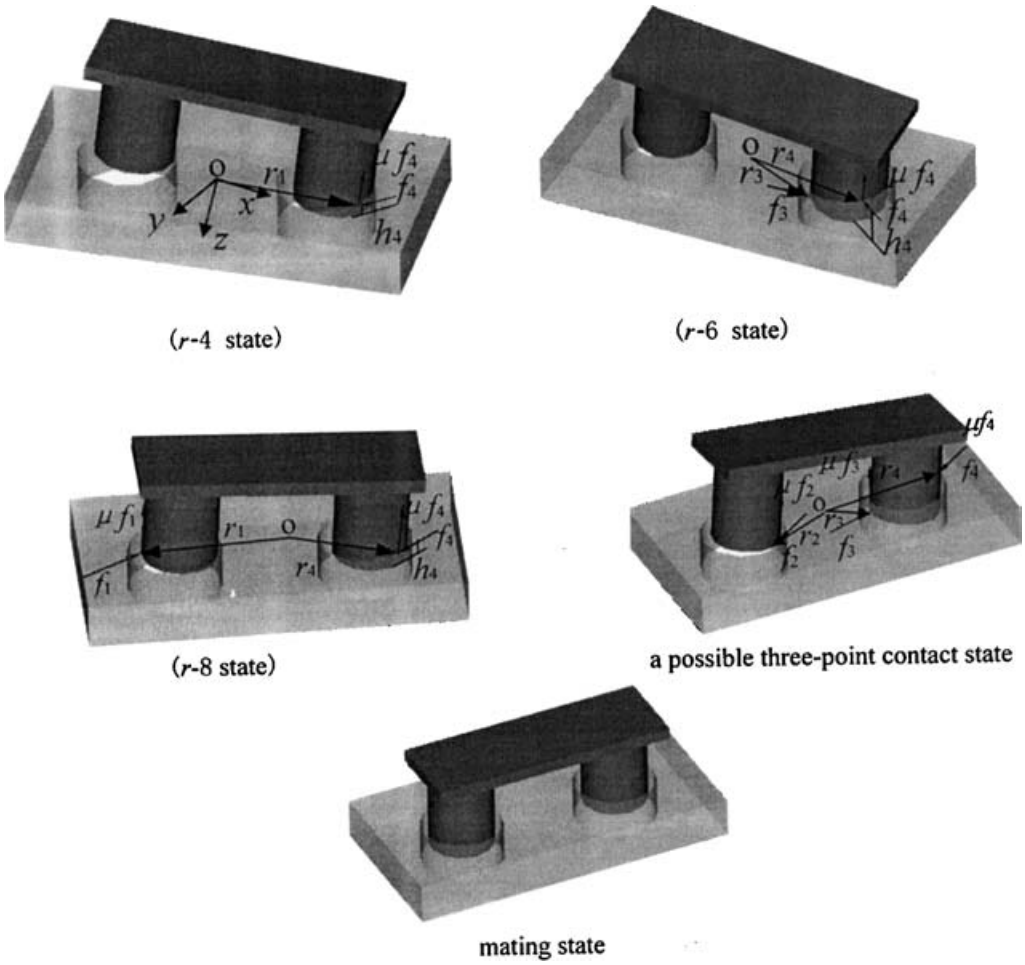



Fig. 3. Assembly states of a dual peg-in-hole in three dimensions.

For example, let pegs tilt to the right. If $i = 1$, a one-point contact state ($r$-4) exists; if $i = 1$ and $i = 4$, a two-point contact state ($r$-8) exists (Fig. 3). In the paper, some states, such as state ($r$-4), state ($r$-6), state ($r$-8), a possible three-point contact state and a mating state are chosen to finish a dual peg-in-hole assembly process. Their three-dimensional charts are shown in Fig. 3.

## 3. GEOMETRIC CONSTRAINT CONDITIONS AND CONTACT STATES ANALYSES

According to the above chosen states (state $r$-4, state $r$-6, state $r$-8, a possible three-point contact state and a mating state), the relations between these states and their geometric constraint conditions are analyzed. Thus, the complexity of the three dimensional dual peg-in-hole can be known. The dimensions of a dual peg and a dual hole are given as follows (Fig. 1): $2r_{P_1} = 2r_{P_2} = 9.9$ mm, $2r_{H_1} = 2r_{H_2} = 10.0$ mm, $D_P = 90.2$ mm, $D_H = 90.25$ mm, $C_1 = C_2 = 0.075$ mm, $\mu = 0.1$.

### *3.1. Two dimensions*

The boundary state of state $r$-4 is shown in Fig. 4. Its geometric constraint condition is

$$\begin{cases} h_0 s\theta_0 + 2r_{P_1} c\theta_0 = 2r_{H_1} \\ h_0 c\theta_0 = 2r_{P_1} s\theta_0 \end{cases} \tag{1}$$

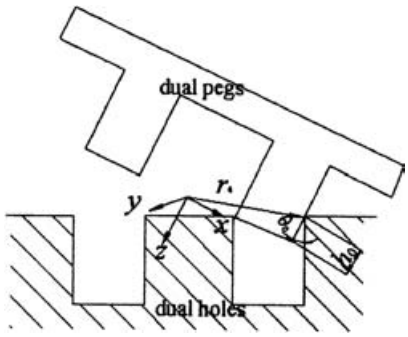



Fig. 4. Boundary state of state $r$-4.

Thus, $\theta_0 = 8.1^\circ$, $h_0 = 1.397$ can be obtained. If $\theta < \theta_0$, state $r$-4 can be reached.

According to Fig. 3, the geometric constraint condition of state $r$-6 in two dimensions can be expressed as,

$$h_4 s\theta + 2r_{P_1} c\theta = 2r_{H_1} \tag{2}$$

The geometric constraint condition of state $r$-8 in two dimensions can be expressed as,

$$h_4 s\theta + \left(D_p + r_{P_2} + r_{P_1}\right) c\theta = \left(D_H + r_{H_2} + r_{H_1}\right) \tag{3}$$

https://doi.org/10.1017/S0263574704000578 Published online by Cambridge University Press

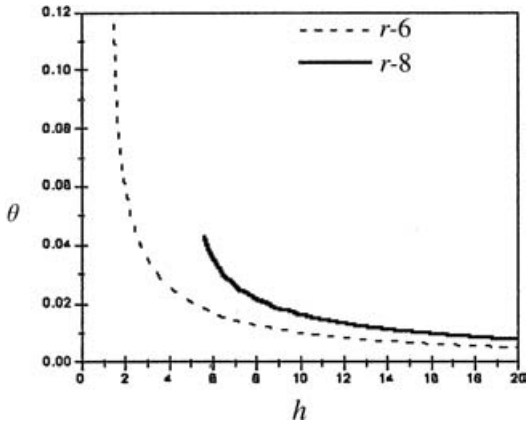



Fig. 5. $\theta$ vs $h$ of state $r$-6 and state $r$-8 in two dimensions.

If Eqs. (2) and (3) can be satisfied simultaneously, a three-point contact state can be reached. Fig. 5 suggests that a three-point contact state is relative to the geometry of assembly objects. At the point where two curves of plots intersect, the three-point contact states can exist. From Fig. 5, we can see that three-point contact states are transient. Here $\theta_0$ and $\theta$ are angles between the axes of a peg and a hole, $h_0$ and $h_1$ are insertion depths.

### *3.2. Three dimensions*

Three-dimensional multiple peg-in-hole problems are more complex than two dimensional peg-in-hole problems. But they have similar geometric constraint conditions. For the boundary state of state $r$-4 in three dimensions, we can obtain:

$$h_0 s\theta_0 + 2r'_{P_1} c\theta_0 = 2r'_{H_1}, \quad r'_{P_1} \le r_{P_1}, \quad r'_{H_1} \le r_{H_1} \tag{4}$$

If $\theta < \theta_0$, state $r$-4 can be reached. For state $r$-6 in three dimensions, we can obtain the following constraint formulas:

$$h_4 s\theta + 2r'_{P_1} c\theta = 2r'_{H_1}, \quad r'_{P_1} \le r_{P_1}, \quad r'_{H_1} \le r_{H_1} \tag{5}$$

For state $r$-8 in three dimensions, we can obtain the following formulas:

$$\begin{aligned} &h_4 s\theta + \left(D'_p + r'_{P_2} + r'_{P_1}\right) c\theta = \left(D'_H + r'_{H_2} + r'_{H_1}\right), \\ &r'_{P_1} \le r_{P_1}, \quad r'_{P_2} \le r_{P_2}, \quad D'_P \le D_p, \quad r'_{H_1} \le r_{H_1}, \\ &\qquad r'_{H_2} \le r_{H_2}, \quad D'_H \le D_H \end{aligned} \tag{6}$$

If constraint conditions are formulas (5) and (6), three-point contact states can be obtained.

Mapping two contact points on the peg to the plane xoy, we can obtain two corresponding points. The distance between these two points is $2r'_{P_1}(2r'_{P_2})$. $2r'_{H_1}$ or $2r'_{H_2}$ represents the distance between two contact points on the left hole or on the right hole, respectively. Mapping one contact point on the left peg and the other contact point on the right peg to the plane xoy, we can obtain two corresponding points. The distance between these two points is $D'_P$. $D'_H$ represents the distance between one contact points on the left hole and the other contact point on the right hole.

According to the analysis of the two dimensional dual peg-in-hole, the following results can be inferred in three dimensions. For different contact geometric dimensions (such as $r'_{P_1}$, $r'_{P_2}$, $D'_P$, $r'_{H_1}$, $r'_{H_2}$ and $D'_H$) of the three dimensional dual peg-in-hole, state $r$-6 and state $r$-8 show different curves, but their change trends are similar. At the point where two curves of state $r$-6 and state $r$-8 intersect, three-point contact states can exist, which are relative to the geometry of assembly objects. This means that three-point contact states, in 3D cases, can exist only when a certain set of conditions are satisfied. They are transient and considered trivial.

## 4. ANALYZING CONTACT FORCE/MOMENT OF THREE DIMENSIONAL DUAL PEG-IN-HOLE BASED ON THE SCREW THEORY

By understanding the physics of assembly processes, one can plan fine motion strategies and guarantee successful operations. An analysis of forces and moments during the three dimensional dual-peg insertion is important in planning fine motions. In order to insert dual pegs into their holes, insertion forces and moments ($F_x$ $F_y$ $F_z$ $M_x$ $M_y$ $M_z$) applied to the pegs have to satisfy a number of conditions. In this section, the conditions on applied forces and moments for maintaining each contact state are derived. Then jamming conditions are obtained. These are basic conditions of fine motions and can avoid unsuccessful insertions. The conditions which guarantee successful insertions can be obtained from the jamming diagrams.

According to a series of chosen contact states in Fig. 3, forces and moments can be described by the screw theory. Because a quasi-static process is assumed, each of the contact states is analyzed from static equilibrium conditions. With the static equilibrium conditions and geometric constraint conditions, the relationship between moments and forces is analyzed. The coordinate system (oxyz) is set up at the center of dual pegs and contact forces are shown in Fig. 3. One-point contact state $r$-4 and two-point contact state $r$-8 are analyzed in detail. The relationship between forces and moments of other contact states can be analyzed similarly (Table II). (i) One-point contact state $r$-4

The wrenches of contact forces in contact points are as follows:

$$\begin{aligned} &(f_4 c\alpha_4 \quad f_4 s\alpha_4 \quad 0 \quad h_4 f_4 s\alpha_4 \quad -h_4 f_4 c\alpha_4 \quad x_4 f_4 s\alpha_4 - y_4 f_4 c\alpha_4). \\ &(0 \quad 0 \quad -\mu f_4 \quad -y_4 \mu f_4 \quad x_4 \mu f_4 \quad 0) \end{aligned}$$

The wrenches of the assembly forces are as follows: ($F_x$ $F_y$ $F_z$ $M_x$ $M_y$ $M_z$).

According to the static equilibrium equations, we can obtain

$$\begin{cases} F_x + f_4 c\alpha_4 = 0 \\ F_y + f_4 s\alpha_4 = 0 \\ F_z - \mu f_4 = 0 \\ M_x + h_4 f_4 s\alpha_4 - y_4 \mu f_4 = 0 \\ M_y - h_4 f_4 c\alpha_4 + x_4 \mu f_4 = 0 \\ M_z + x_4 f_4 s\alpha_4 - y_4 f_4 c\alpha_4 = 0 \end{cases} \tag{7}$$

https://doi.org/10.1017/S0263574704000578 Published online by Cambridge University Press

Table II. Force/moment of contact states about the three dimensional dual peg-in-hole.

| Three dimensional contact states | Force/moment of contact states |
|---|---|
| One-point contact states | |
| ($k$-1) | $\begin{cases}\frac{F_x}{F_z}=-\frac{c\alpha_1}{\mu}\\ \frac{M_y}{F_z}=j\frac{h_1c\alpha_1}{\mu}-x_1\end{cases}\quad\begin{cases}\frac{F_y}{F_z}=-\frac{s\alpha_1}{\mu}\\ \frac{M_x}{F_z}=-j\frac{h_1s\alpha_1}{\mu}+y_1\end{cases}$ |
| ($k$-2) | $\begin{cases}\frac{F_x}{F_z}=-\frac{c\alpha_2}{\mu}\\ \frac{M_y}{F_z}=(1-j)\frac{h_2c\alpha_2}{\mu}-x_2\end{cases}\quad\begin{cases}\frac{F_y}{F_z}=-\frac{s\alpha_2}{\mu}\\ \frac{M_x}{F_z}=-(1-j)\frac{h_2s\alpha_2}{\mu}+y_2\end{cases}$ |
| ($k$-3) | $\begin{cases}\frac{F_x}{F_z}=-\frac{c\alpha_3}{\mu}\\ \frac{M_y}{F_z}=j\frac{h_3c\alpha_3}{\mu}-x_3\end{cases}\quad\begin{cases}\frac{F_y}{F_z}=-\frac{s\alpha_3}{\mu}\\ \frac{M_x}{F_z}=-j\frac{h_3s\alpha_3}{\mu}+y_3\end{cases}$ |
| ($k$-4) | $\begin{cases}\frac{F_x}{F_z}=-\frac{c\alpha_4}{\mu}\\ \frac{M_y}{F_z}=(1-j)\frac{h_4c\alpha_4}{\mu}-x_4\end{cases}\quad\begin{cases}\frac{F_y}{F_z}=-\frac{s\alpha_4}{\mu}\\ \frac{M_x}{F_z}=-(1-j)\frac{h_4s\alpha_4}{\mu}+y_4\end{cases}$ |
| Two-point contact states | |
| ($k$-5) | $\frac{M_y}{DF_z}=-\frac{\mu}{c\alpha_1-c\alpha_2}\left[\frac{x_2-x_1}{D}+j\frac{h_1c\alpha_1}{\mu D}-(1-j)\frac{h_2c\alpha_2}{\mu D}\right]\frac{F_x}{F_z}+\frac{\mu x_1c\alpha_2-\mu x_2c\alpha_1-jh_1c\alpha_1c\alpha_2+(1-j)h_2c\alpha_1c\alpha_2}{\mu D(c\alpha_1-c\alpha_2)}$<br>$\frac{M_x}{DF_z}=-\frac{\mu}{s\alpha_1-s\alpha_2}\left[-\frac{y_2-y_1}{D}-j\frac{h_1s\alpha_1}{\mu D}+(1-j)\frac{h_2s\alpha_2}{\mu D}\right]\frac{F_y}{F_z}+\frac{-\mu y_1s\alpha_2+\mu y_2s\alpha_1+jh_1s\alpha_1s\alpha_2-(1-j)h_2s\alpha_1s\alpha_2}{\mu D(s\alpha_1-s\alpha_2)}$ |
| ($k$-6) | $\frac{M_y}{DF_z}=-\frac{\mu}{c\alpha_3-c\alpha_4}\left[\frac{x_4-x_3}{D}+j\frac{h_3c\alpha_3}{\mu D}-(1-j)\frac{h_4c\alpha_4}{\mu D}\right]\frac{F_x}{F_z}+\frac{\mu x_3c\alpha_4-\mu x_4c\alpha_3-jh_3c\alpha_3c\alpha_4+(1-j)h_4c\alpha_3c\alpha_4}{\mu D(c\alpha_3-c\alpha_4)}$<br>$\frac{M_x}{DF_z}=-\frac{\mu}{s\alpha_3-s\alpha_4}\left[-\frac{y_4-y_3}{D}-j\frac{h_3s\alpha_3}{\mu D}-(1-j)\frac{h_4s\alpha_4}{\mu D}\right]\frac{F_y}{F_z}+\frac{-\mu y_3s\alpha_4+\mu y_4s\alpha_3+jh_3s\alpha_3s\alpha_4-(1-j)h_4s\alpha_3s\alpha_4}{\mu D(s\alpha_3-s\alpha_4)}$ |
| ($k$-7) | $\frac{M_y}{DF_z}=\frac{\mu}{c\alpha_1-c\alpha_3}\left(\frac{x_1-x_3}{D}+j\frac{-h_1c\alpha_1+h_3c\alpha_3}{\mu D}\right)\frac{F_x}{F_z}+\frac{x_1\mu c\alpha_3-x_3\mu c\alpha_1+j(-h_1c\alpha_1c\alpha_3+h_3c\alpha_1c\alpha_3)}{\mu D(c\alpha_1-c\alpha_3)}$<br>$\frac{M_x}{DF_z}=-\frac{\mu}{s\alpha_1-s\alpha_3}\left(\frac{y_1-y_3}{D}+j\frac{-h_1s\alpha_1+h_3s\alpha_3}{\mu D}\right)\frac{F_y}{F_z}+\frac{y_2\mu s\alpha_1-y_1\mu s\alpha_3+j(h_1s\alpha_1s\alpha_3-h_3s\alpha_1s\alpha_3)}{\mu D(s\alpha_1-s\alpha_3)}$ |
| ($k$-8) | $\frac{M_y}{DF_z}=-\frac{\mu}{c\alpha_1-c\alpha_4}\left[\frac{x_4-x_1}{D}+j\frac{h_1c\alpha_1}{\mu D}-(1-j)\frac{h_4c\alpha_4}{\mu D}\right]\frac{F_x}{F_z}+\frac{\mu x_1c\alpha_4-\mu x_4c\alpha_1-jh_1c\alpha_1c\alpha_4+(1-j)h_4c\alpha_1c\alpha_4}{\mu D(c\alpha_1-c\alpha_4)}$<br>$\frac{M_x}{DF_z}=-\frac{\mu}{s\alpha_1-s\alpha_4}\left[-\frac{y_4-y_1}{D}-j\frac{h_1s\alpha_1}{\mu D}+(1-j)\frac{h_4s\alpha_4}{\mu D}\right]\frac{F_y}{F_z}+\frac{-\mu y_1s\alpha_4+\mu y_4s\alpha_1+jh_1s\alpha_1s\alpha_4-(1-j)h_4s\alpha_1s\alpha_4}{\mu D(s\alpha_1-s\alpha_4)}$ |
| ($k$-9) | $\frac{M_y}{DF_z}=-\frac{\mu}{c\alpha_3-c\alpha_2}\left[\frac{x_2-x_3}{D}+j\frac{h_3c\alpha_3}{\mu D}-(1-j)\frac{h_2c\alpha_2}{\mu D}\right]\frac{F_x}{F_z}+\frac{\mu x_3c\alpha_2-\mu x_2c\alpha_3-jh_3c\alpha_3c\alpha_2+(1-j)h_2c\alpha_2c\alpha_3}{\mu D(c\alpha_3-c\alpha_2)}$<br>$\frac{M_x}{DF_z}=-\frac{\mu}{s\alpha_3-s\alpha_2}\left[-\frac{y_2-y_3}{D}-j\frac{h_3s\alpha_3}{\mu D}+(1-j)\frac{h_2s\alpha_2}{\mu D}\right]\frac{F_y}{F_z}+\frac{-\mu y_3s\alpha_2+\mu y_2s\alpha_3+jh_3s\alpha_3s\alpha_2-(1-j)h_2s\alpha_2s\alpha_3}{\mu D(s\alpha_3-s\alpha_2)}$ |
| ($k$-10) | $\frac{M_y}{DF_z}=\frac{\mu}{c\alpha_2-c\alpha_4}\left(\frac{x_2-x_4}{D}+(1-j)\frac{-h_2c\alpha_2+h_4c\alpha_4}{\mu D}\right)\frac{F_x}{F_z}+\frac{\mu x_2c\alpha_4-\mu x_4c\alpha_2+(1-j)(-h_2c\alpha_2c\alpha_4+h_4c\alpha_2c\alpha_4)}{\mu D(c\alpha_2-c\alpha_4)}$<br>$\frac{M_x}{DF_z}=-\frac{\mu}{s\alpha_2-s\alpha_4}\left(\frac{y_2-y_4}{D}+(1-j)\frac{-h_2s\alpha_2+h_4s\alpha_4}{\mu D}\right)\frac{F_y}{F_z}+\frac{\mu y_4s\alpha_2-\mu y_2s\alpha_4+(1-j)(h_2s\alpha_2s\alpha_4-h_4s\alpha_2s\alpha_4)}{\mu D(s\alpha_2-s\alpha_4)}$ |

When pegs tilt to the left, $k$ stands for $l$ and $j=1$. When pegs tilt to the right, $k$ stands for $r$ and $j=0$.

Thus, we can obtain the following relationship equations,

$$\begin{cases}\dfrac{F_x}{F_z}=-\dfrac{c\alpha_4}{\mu}\\ \dfrac{M_y}{F_z}=\dfrac{h_4c\alpha_4}{\mu}-x_4\end{cases}\tag{8}$$

$$\begin{cases}\dfrac{F_y}{F_z}=-\dfrac{s\alpha_4}{\mu}\\ \dfrac{M_x}{F_z}=-\dfrac{h_4s\alpha_4}{\mu}+y_4\end{cases}\tag{9}$$

where $\alpha_4\in[90^\circ\ 270^\circ]$, $r_4$: $(x_4\ y_4\ -h_4)$.

(ii) two-point contact state $r$-8

The wrenches of contact forces in contact points are as follows,

$$\begin{array}{l}(f_1c\alpha_1\quad f_1s\alpha_1\quad 0\quad 0\quad 0\quad x_1f_1s\alpha_1-y_1f_1c\alpha_1)\\ (0\quad 0\quad -\mu f_1\quad -y_1\mu f_1\quad x_1\mu f_1\quad 0)\\ (f_4c\alpha_4\quad f_4s\alpha_4\quad 0\quad h_4f_4s\alpha_4\quad -h_4f_4c\alpha_4\quad x_4f_4c\alpha_4-y_4f_4c\alpha_4)\\ (0\quad 0\quad -\mu f_4\quad -y_4\mu f_4\quad x_4\mu f_4\quad 0)\end{array}$$

The wrenches of the assembly forces are as follows: $(F_x\ F_y\ F_z\ M_x\ M_y\ M_z)$.

According to the static equilibrium equations, the following equations can be obtained,

$$\frac{M_x}{DF_z}=-\frac{\mu}{c\alpha_4-c\alpha_1}\left[\frac{x_1-x_4}{D}+\frac{h_4c\alpha_4}{\mu D}\right]\frac{F_x}{F_z}+\frac{\mu x_4c\alpha_1-\mu x_1c\alpha_4-h_4c\alpha_1c\alpha_4}{\mu D(c\alpha_4-c\alpha_1)}\tag{10}$$

https://doi.org/10.1017/S0263574704000578 Published online by Cambridge University Press

$$\frac{M_x}{DF_z} = -\frac{\mu}{s\alpha_4 - s\alpha_1}\left[-\frac{y_1 - y_4}{D} - \frac{h_4 s\alpha_4}{\mu D}\right]\frac{F_y}{F_z} + \frac{-\mu y_4 s\alpha_1 + \mu y_1 s\alpha_4 + h_4 s\alpha_1 s\alpha_4}{\mu D(s\alpha_4 - s\alpha_1)} \quad (11)$$

Eqs. (10) and (11) show linear relations. For Eq. (10), when $\frac{F_x}{F_z} = -\frac{c\alpha_1}{\mu}$, we can write $\frac{M_y}{DF_z} = -\frac{x_1}{D}$. When $\frac{F_x}{F_z} = -\frac{c\alpha_4}{\mu}$, we can write $\frac{M_y}{DF_z} = \frac{h_4 c\alpha_4}{\mu D} - \frac{x_4}{D}$. For Eq. (11), when $\frac{F_y}{F_z} = -\frac{s\alpha_1}{\mu}$, we can write $\frac{M_x}{DF_z} = \frac{y_1}{D}$. When $\frac{F_y}{F_z} = -\frac{s\alpha_4}{\mu}$, we can write $\frac{M_x^{\mu}}{DF_z} = -\frac{h_4 s\alpha_4}{\mu D} + \frac{y_4}{D}$. where $\alpha_1 \in [0^\circ\ 90^\circ] \cup [270^\circ\ 360^\circ]$, $\alpha_4 \in [90^\circ\ 270^\circ]$, $r_1$: $(x_1\ y_1\ 0)$, $r_4$: $(x_4\ y_4\ -h_4)$.

## 5. JAMMING DIAGRAMS OF THREE DIMENSIONAL DUAL PEG-IN-HOLE

Because the relationship between forces and moments is not proper, pegs are stuck in the holes and jamming appears.

### *5.1. Jamming diagrams*

In this section, according to the relations between $\frac{M_y}{F_z}$ and $\frac{F_x}{F_z}$, $\frac{M_x}{F_z}$ and $\frac{F_y}{F_z}$, we can obtain three kinds of jamming diagrams about three-dimensional dual peg-in-hole problems (Fig. 6):

(a) $\frac{M_y}{DF_z} \propto \frac{F_x}{F_z}$;

(b) $\frac{M_x}{DF_z} \propto \frac{F_y}{F_z}$, $\alpha_1 \in [0^\circ\ \ 90^\circ]$, $\alpha_3 \in [0^\circ\ \ 90^\circ]$, $\alpha_2 \in [180^\circ\ \ 270^\circ]$, $\alpha_4 \in [180^\circ\ \ 270^\circ]$;

(c) $\frac{M_x}{DF_z} \propto \frac{F_y}{F_z}$, $\alpha_1 \in [270^\circ\ \ 360^\circ]$, $\alpha_3 \in [270^\circ\ \ 360^\circ]$, $\alpha_2 \in [90^\circ\ \ 180^\circ]$, $\alpha_4 \in [90^\circ\ \ 180^\circ]$.

Table II lists the force/moment conditions for 20 possible contact states. Fig. 6 shows the jamming diagrams of the three dimensional dual-peg problem with these contact states. When the force/moment conditions of all possible contact states of the three dimensional dual-peg insertion problem are plotted in the force/moment space, the plots form a closed boundary which separates the force/moment space into two spaces; statically unstable space, and jamming space. The unstable space is the area enclosed by the boundary, and represents the conditions on the applied forces and moments that cause the pegs to unstably fall into the holes. The jamming space, on the other hand, is the area outside the boundary, and represents the force/moment conditions in which the pegs appear stuck in the holes because the applied forces and moments cannot overcome the net forces and moments due to frictional contact forces (Fig. 6). The jamming diagrams can supply us some useful insertion information. If the conditions on the applied forces and moments fall into the unstable space, the pegs can unstably fall into the holes and the continuity of insertion can be guaranteed. Since all 20 contact states cannot exist at a particular geometric condition, each jamming diagram representing a particular insertion problem is constructed from only some of the straight lines shown in Fig. 6. When

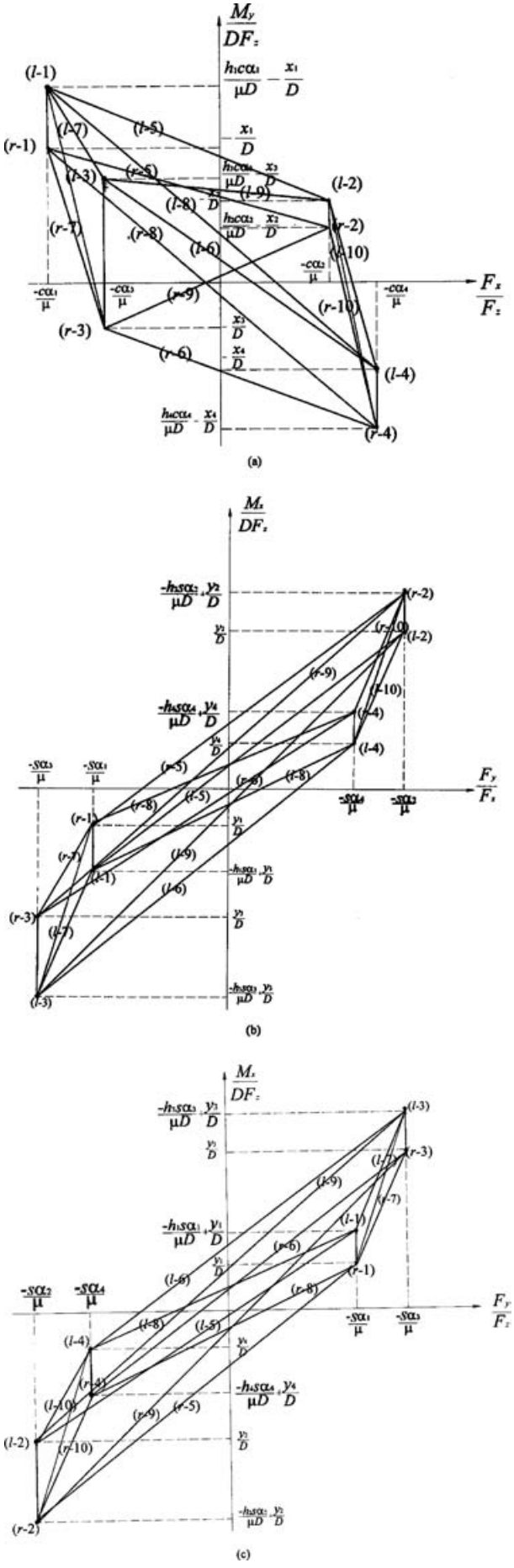



Fig. 6. Jamming diagrams.

https://doi.org/10.1017/S0263574704000578 Published online by Cambridge University Press

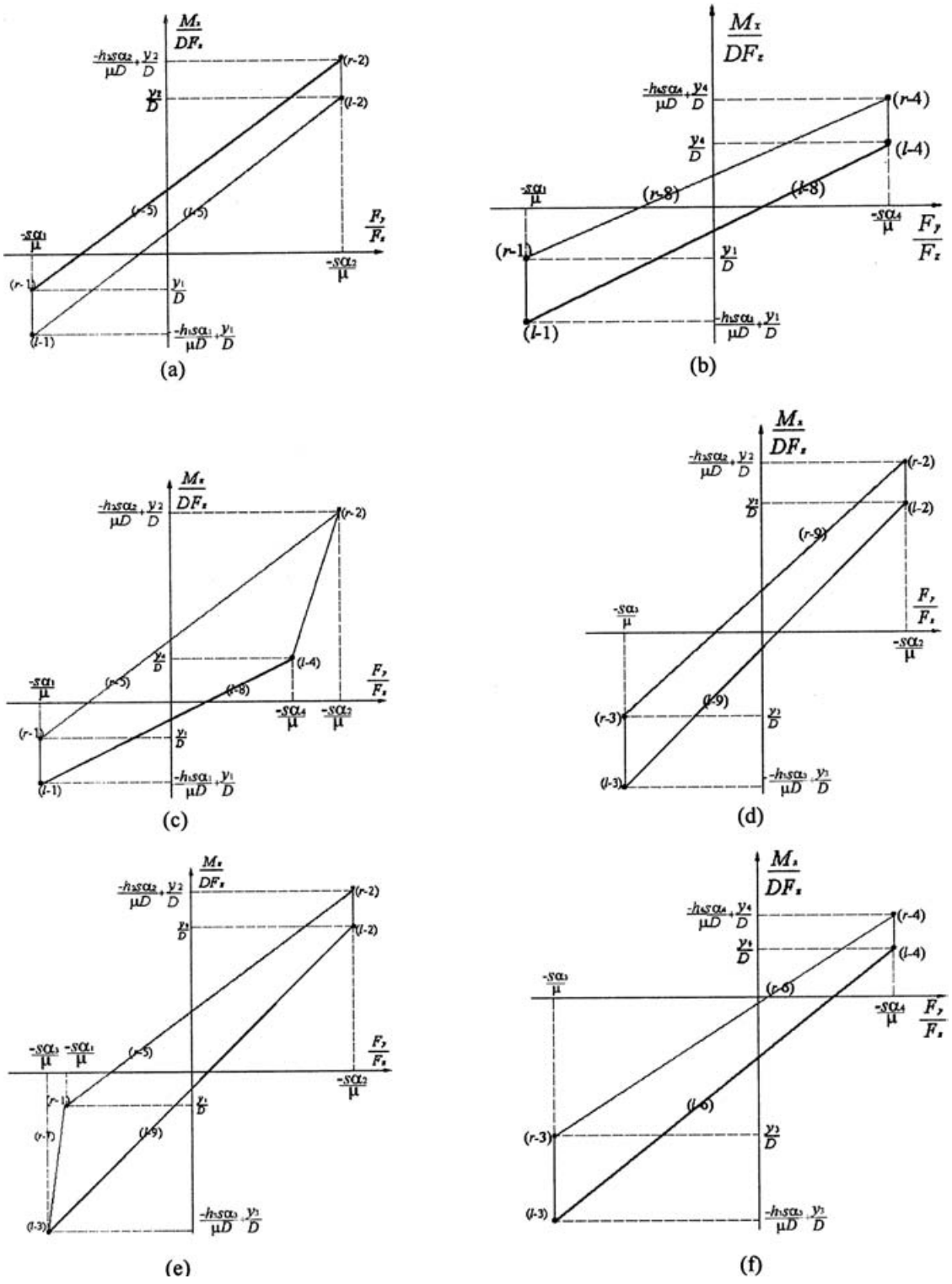



Fig. 7. For caption see next page.

the geometric dimensions and the insertion depth are known, some possible contact states can be formed and some possible jamming diagrams can be obtained (Fig. 7).

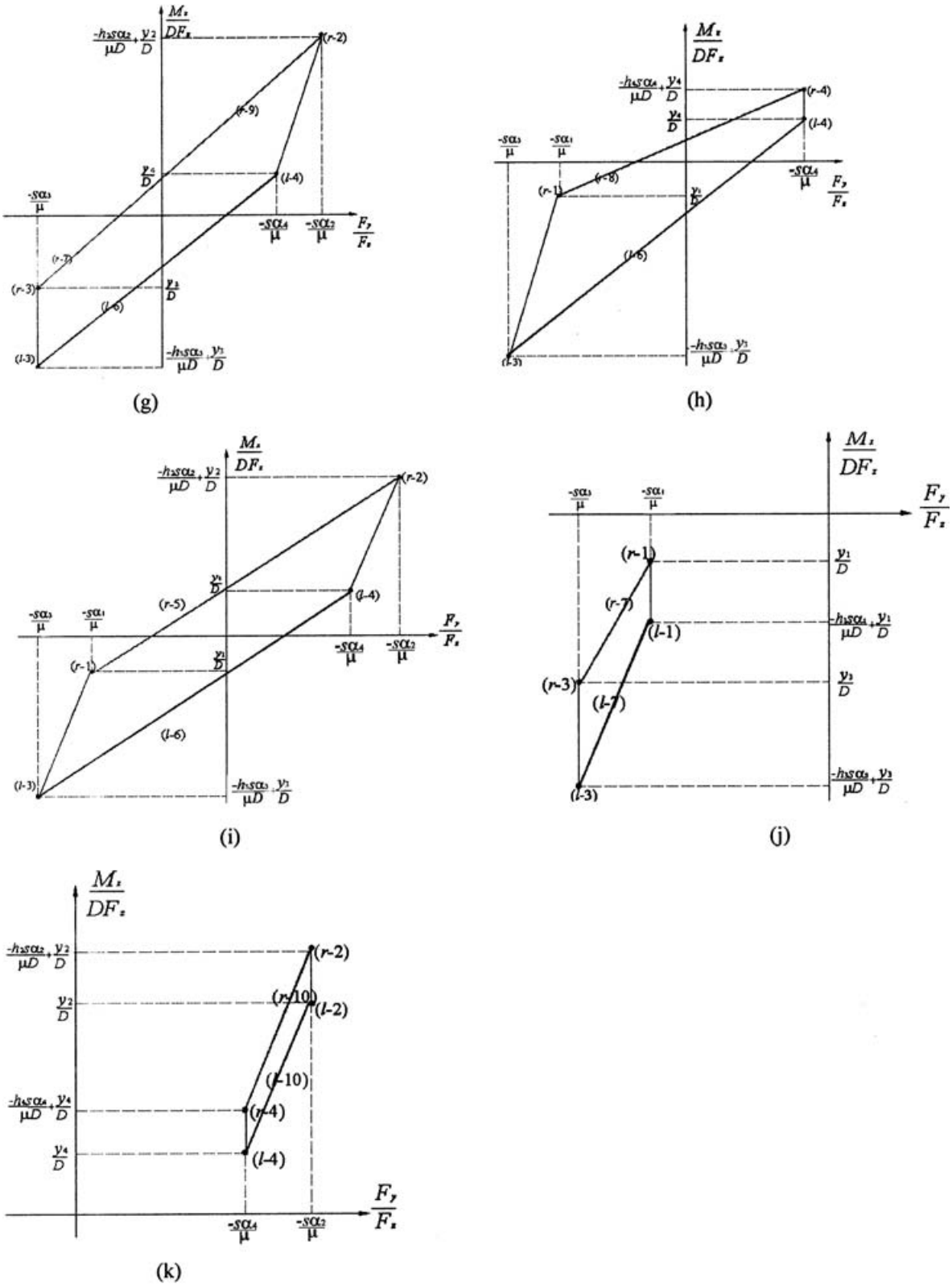
*5.2. 11 kinds of possible jamming diagrams*

For three kinds of jamming diagrams in Fig. 6, each has 11 kinds of possible jamming diagrams. For example, in Fig. 6(b), for a particular insertion condition, the possible jamming diagrams can be constructed by joining four corresponding lines forming an enclosed region (Fig. 7). In Fig. 7, vertices of the quadrangle represent one-point contact states, such as ($l$-1), ($l$-2), ($r$-1), ($r$-2) in Fig. 7(a). Lines of the quadrangle represent two-point contact states, such as ($l$-5), ($r$-5) in Fig. 7(a).

## 6. EXPERIMENT

An experiment has been conducted to verify the foregoing analyses. The geometric dimensions of a dual peg-in-hole are set in section 3 (Fig. 1).

https://doi.org/10.1017/S0263574704000578 Published online by Cambridge University Press




$$\frac{M_x}{DF_z} \propto \frac{F_y}{F_z},\ \alpha_1 \in [0°\ \ 90°], \alpha_3 \in [0°\ \ 90°], \alpha_2 \in [180°\ \ 270°], \alpha_4 \in [180°\ \ 270°]$$

Fig. 7. Possible jamming diagrams.

https://doi.org/10.1017/S0263574704000578 Published online by Cambridge University Press



Fig. 8. Contact state (pegs tilt to right).

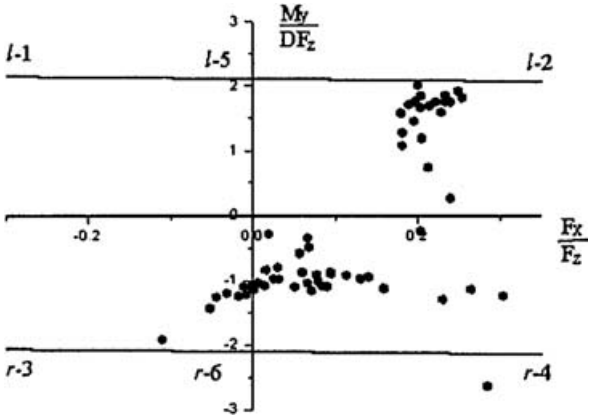



Fig. 9. A jamming diagram.

*6.1. Experiment setup*

In the experiment presented in this section, a six-degree of freedom Motoman robot and a force/moment sensor are used. Correspondingly, forces and moments are sampled. The shape of assembly objects and the apparatus used to verify contacts states and geometric relations of the assembly process are shown in Fig. 8.

*6.2. Analyses of experiment result (jamming diagram)*

After finishing a series of chosen states about the dual peg-in-hole, some forces and moments can be sampled. With these data, the relationship between forces and moments can be calculated. Thus we can infer whether they fall into the jamming spaces. From the above analysis of jamming diagrams, if the conditions of applied forces and moments don't fall into the jamming spaces, pegs are not stuck in the whole assembly process and can fall into the holes. Using the data of these states, we can see that these data which are described by black points fall into the unstable space ($l$-1, $l$-5, $l$-2, $r$-3, $r$-6, $r$-4) (Fig 9). This shows that dual pegs fall into dual holes during the assembly process. According to the above analysis, jamming diagram ($l$-1, $l$-5, $l$-2, $r$-3, $r$-6, $r$-4) can be obtained, which verifies the above content.

## 7. CONCLUSIONS

In this paper, the jamming of a dual peg-in-hole insertion in three dimensions is analyzed in detail. Firstly, 20 contact states of the three dimensional dual-peg are enumerated and geometric conditions are derived. Secondly, the contact forces are described by the screw theory in three dimensions. With the static equilibrium equations, the relationship between forces and moments for maintaining each contact state is derived. Thirdly, the jamming diagrams of the three dimensional dual peg-in-hole are presented. 11 different types of possible jamming diagrams for one of three jamming diagrams are identified. These jamming diagrams can be used to plan fine motion strategies for successful insertions. Finally, an experiment of a dual peg-in-hole is presented. Experimental results show the applicability of the analyses for jamming. In addition, they also show that the assembly process in six degrees of freedom is more complex than that for planar motion. The above analyses are the theoretical bases for multiple peg-in-hole insertions.

## Acknowledgements

This work was supported by the National Natural Science Foundation of China under Grant 50305021 and Grant 50390063.

## References

1. J. Xiao, "Automatic determination of topological containts in the presence of sensing uncertainties", *Proc. of IEEE Int. Conf. on Robotics and Automation*, Atlanta, May (1993), pp. 65–70.
2. J. Xiao and Xuerong Ji, "Automatic generation of high-level contact state space", *Int. J. Robotics Research* **20**(7), 584–606 (2001).
3. S. N. Simunovic, "Force information in assembly process", *Proc. of the 5th Int' l Symposium on Industrial Robots*, Chicago Illinois (1972), pp. 113–126.
4. D. E. Whitney, "Quasi-static assembly of compliantly supported rigid parts", *ASME J. of Dynamic Systems, Measurement, and Control* **104**, 65–77 (1982).
5. R. H. Sturges, "A three-dimensional assembly task quantification with application to machine dexterity", *Int. J. Robotics Research* **7**(1), 34–78 (1988).
6. R. H. Sturges and S. Laowattana, "Virtual wedging in three-dimensional peg insertion tasks", *Journal of Mechanical Design* **118**, 99–105 (1996).
7. R. H. Sturges and S. Laowattana, "Design of an orthogonal compliance for polygonal peg insertion", *Journal of Mechanical Design* **118**, 106–114 (1996).
8. C. J. Tsaprounis and N. Aspragathos, "Contact point identification in robot assembly strategies under uncertainty", *Robotica*, **16**, Part 6, 679–690 (1998).
9. T. Arai et al, "Hole search planning for peg-in-hole problem", *Manufacturing Systems* **26**(2), 119–124 (1997).
10. B. J. McCarragher and H. Asada, "The discrete event control of robotic assembly tasks", *J. of Dynamic System, Measurement and Control* **117**(3), 384–393 (1995).
11. K. Sathirakul and R. H. Sturges, "Jamming conditions for multiple peg-in-hole assemblies", *Robotica* **16**, Part , 329–345 (1998).
12. S. Rossitza and B. Damel, "Three-dimensional simulation of accommodation", *Assembly Automation* **18**(4), 291–301 (1998).
13. R. H. Sturges and K. Sathirakul, "Modeling multiple peg-in-hole insertion tasks", *Proc. of the Japan/USA Symposium on Flexible Automation* (1996), pp. 819–821.
14. Y. Q. Fei and X. F. Zhao, "An assembly process modeling and analysis for robotic multiple peg-in-hole", *Journal of Intelligent and Robotic Systems* **36**(2), 175–189 (2003).

https://doi.org/10.1017/S0263574704000578 Published online by Cambridge University Press